European Journal of Pharmaceutical Sciences 125 (2018) 110–119

Contents lists available at ScienceDirect

European Journal of Pharmaceutical Sciences

journal homepage: www.elsevier.com/locate/ejps

Combined use of biocompatible nanoemulsions and solid microneedles to improve transport of a model NSAID across the skin: In vitro and in vivo studies

Tanja Ilić[a], Sanela Savić[b], Bojan Batinić[c], Bojan Marković[d], Markus Schmidberger[e], Dominique Lunter[e], Miroslav Savić[f], Snežana Savić[a,*]

[a] Department of Pharmaceutical Technology and Cosmetology, Faculty of Pharmacy, University of Belgrade, Belgrade, Serbia
[b] DCP Hemigal, Leskovac, Serbia
[c] Department of Physiology, Faculty of Pharmacy, University of Belgrade, Belgrade, Serbia
[d] Department of Pharmaceutical Chemistry, Faculty of Pharmacy, University of Belgrade, Belgrade, Serbia
[e] Institut für Pharmazeutische Technologie, Eberhard-Karls Universität, D-72076 Tübingen, Germany
[f] Department of Pharmacology, Faculty of Pharmacy, University of Belgrade, Belgrade, Serbia

ARTICLE INFO

Keywords:
Aceclofenac
Stainless steel microneedles
In vitro drug release
In vitro skin permeation
Differential stripping
In vivo pharmacokinetics

ABSTRACT

This study aimed to investigate the potential of lecithin-based nanoemulsions costabilized by sucrose esters, with and without skin pretreatment with stainless steel microneedles, to improve delivery of aceclofenac, as a model drug, into/across the skin. The characterization revealed favorable droplet size (about 180 nm), narrow size distribution (< 0.15), high surface charge (about −40 mV) and satisfying long-term stability (one year at 4 ± 1 °C) of the formulation costabilized by sucrose palmitate, demonstrating a similar trend observed for the reference stabilized by widely used lecithin/polysorbate 80 combination. In vitro release/permeation testing and differential stripping on the porcine ear proved the superiority of the sucrose ester- over polysorbate-based nanoemulsion. However, in vitro findings were not fully indicative of the in vivo performances – no significant differences were observed between investigated formulations in pharmacokinetic profile and total amount of aceclofenac deposited in the rat skin 24 h after dosing, simultaneously pointing to delayed aceclofenac delivery into the systemic circulation. In addition, the ratio of plasma concentrations of aceclofenac and its major metabolite in rats, diclofenac, was remarkably changed after topical application of tested nanoemulsions compared to intravenous administration of aceclofenac solution. Finally, skin pretreatment with microneedles improved aceclofenac delivery into/across the rat skin from tested formulations, resulting in 1.4–2.1-fold increased bioavailability and 1.2–1.7-fold enhanced level of aceclofenac retained in the skin, as measured 24 h after administration. Moreover, the plasma concentrations of aceclofenac 24 h after application of tested formulations (lecithin/sucrose palmitate vs. lecithin/polysorbate 80) combined with microneedles (173.37 ± 40.50 ng/ml vs. 259.23 ± 73.18 ng/ml) were significantly higher than those obtained through intact skin (105.69 ± 19.53 ng/ml vs. 88.38 ± 14.46 ng/ml). However, obtained results suggest that combination of microneedles and sucrose palmitate-costabilized nanoemulsion could be useful to attain higher skin concentration, while combination of microneedles with polysorbate 80-costabilized nanoemulsion could be a preferable option for enhancing drug delivery into the bloodstream.

1. Introduction

Over the past decades, a relatively high incidence of serious gastrointestinal adverse effects associated with chronic oral administration of non-steroidal anti-inflammatory drugs (NSAIDs), along with often limited therapeutic efficacy of marketed topical NSAID products, has enforced intensive research efforts towards exploring different percutaneous penetration enhancement technologies aiming to ensure effective treatment of various musculoskeletal disorders via skin. Considering that the success of topical NSAID therapy predominantly depends on the drug's capability to penetrate the stratum corneum (SC) layer in sufficiently high amount to exert its clinical effect, formulators

* Corresponding author at: Department of Pharmaceutical Technology and Cosmetology, Faculty of Pharmacy, University of Belgrade, Vojvode Stepe 450, 11221 Belgrade, Serbia.
E-mail address: snexs@pharmacy.bg.ac.rs (S. Savić).

https://doi.org/10.1016/j.ejps.2018.09.023
Received 23 June 2018; Received in revised form 8 September 2018; Accepted 30 September 2018
Available online 02 October 2018
0928-0987/

have increasingly turned to a range of nanotechnology-based drug delivery systems for enhancing transport of NSAIDs across the skin (Cevc and Vierl, 2010; Jana et al., 2014; Raza et al., 2014; Todosijević et al., 2015). Among different nanocarriers proposed, considerable attention, during the last decade, has been focused on nanoemulsions, because of their distinct advantages such as high solubilization capacity for lipophilic drugs, satisfying physical stability, high skin friendliness, relatively ease manufacture and scale-up (Isailović et al., 2016; Klang et al., 2015; Singh et al., 2017). Additionally, owing to enhanced drug concentration gradient, penetration of nanodroplets into the hair follicles, and skin barrier perturbation by surfactants employed for stabilization, an improved skin uptake of NSAIDs could be expected with nanoemulsion systems (Klang et al., 2015; Khandavilli and Panchagnula, 2007).

In this respect, the selection of proper excipients, particularly surfactant/cosurfactant mixture, is of paramount importance for the formation and stability of nanoemulsions and, also, for the efficient skin delivery of incorporated drug (Klang and Valenta, 2011; Milić et al., 2017). Although polyethoxylated non-ionic surfactants (e.g., polysorbate 80 (P80)) exhibit satisfying functionality in the classical lecithin-based nanoemulsions, concerns regarding their safety and in vivo fate have led to a growing interest in application of biodegradable, non-irritant and environmental-friendly surfactants, such as sucrose esters (SEs) which can act as skin penetration enhancer, as well (Hoeller et al., 2009; Isailović et al., 2016; Szűts and Szabó-Révész, 2012). Accordingly, in order to attain improved delivery of aceclofenac (ACF) as a model NSAID across the skin, we have recently developed, characterized, and with the aid of experimental design optimized, novel nanoemulsions using egg lecithin and sucrose palmitate (SP) and/or sucrose stearate (SS) as emulsifiers, and discussed in detail the impact of stabilizer mixture composition on skin uptake of ACF (Isailović et al., 2016). The obtained results showed that novel SEs-based nanoemulsions significantly enhanced cutaneous penetration of ACF compared to the reference costabilized by P80, simultaneously exhibiting satisfying preliminary skin irritation profile (Isailović et al., 2016); however, more elaborate study was needed to assess their suitability for dermal/transdermal delivery of ACF. Here, it is important to note that although certain systemic activity of antiinflammatory drugs formulated in nanoemulsions was observed (Friedman et al., 1995), generally, literature data about delivering drugs transdermally, using classical submicron emulsion systems, is scarce (Klang et al., 2015).

A further alternative for improving permeation of NSAIDs across the skin presents the temporary disruption of SC using the minimally invasive and painless physical enhancers, such as solid microneedles. After inserting and removing, microneedle arrays create aqueous microchannels in the outer skin layers, through which drug molecules applied onto the skin can more easily transport (Coulman et al., 2009; Kim et al., 2012; Zhang et al., 2010). Making certain connection with nanoparticles, which combination with microneedles has been extensively studied (Larrañeta et al., 2016), it is intuitive to assume that microconduits formed by microneedle application might enable the penetration of intact nanodroplets into the skin, thus ensuring the efficient intradermal/transdermal delivery of incorporated drug. However, it should be kept in mind that the skin permeability and the degree of drug delivery using nanoemulsion/microneedles combination can be influenced by numerous parameters related to the properties of microneedle arrays and nanoemulsion formulation, as well (Coulman et al., 2009; Milewski et al., 2010; Zhang et al., 2010).

Based on above considerations, the present study aimed to deepen the acquired knowledge about recently developed SE-based nanoemulsions (Isailović et al., 2016) as vehicles for improved delivery of ACF, as a model NSAID, across the skin. For this purpose, three most promising ACF-loaded nanoemulsion formulations differing in the ratio of egg lecithin, SP and SS, within the equal amount of stabilizers' blend (Table 1), were compared mutually, and with the reference stabilized with widely used lecithin/P80 combination, regarding their physicochemical properties, long-term stability and in vitro drug release/permeation profiles. Additionally, in order to identify the preferable factors contributing to improved delivery of ACF into/through the skin from developed nanoemulsions, the influence of the stabilizers' mixture composition on the extent of ACF follicular uptake was also investigated using differential stripping technique on porcine ear skin. Finally, hypothesizing that microneedle pretreatment (physical enhancing effect) may further facilitate transport of ACF across the skin, we investigated the plasma pharmacokinetics of ACF in rats (including quantification of ACF amount retained in the skin) after topical administration of formulated nanoemulsions, with and without skin perforation using commercially available stainless steel microneedles (AdminPatch® microneedle arrays). To the best of our knowledge, this is the first study showing the effect of combined use of nanoemulsions and solid microneedles on the ACF delivery in vivo, into the skin and through the skin into the systemic circulation.

Table 1
Composition of investigated nanoemulsions.

Composition (%, w/w)	L_2P_2/ L_2P_2A[a]	$L_{1.5}S_{0.5}P_2$/ $L_{1.5}S_{0.5}P_2A$[a]	$L_1S_1P_2$/ $L_1S_1P_2A$[a]	L_2P80_2/ L_2P80_2A[a]
Oil phase				
Medium chain triglycerides	10	10	10	10
Castor oil	10	10	10	10
Butylhydroxytoluene	0.05	0.05	0.05	0.05
Egg lecithin	2	1.5	1	2
Aceclofenac	–/1	–/1	–/1	–/1
Aqueous phase				
Sucrose palmitate P-1670	2	2	2	/
Sucrose stearate S-970	/	0.5	1	/
Polysorbate 80	/	/	/	2
Ultrapure water to	100	100	100	100

[a] Unique code for identifying the qualitative and quantitative composition of tested nanoemulsions (for example, L with subscript 1 stands for 1% of egg lecithin, S with subscript 1 stands for 1% of sucrose stearate, P with subscript 2 for 2% of sucrose palmitate, P80 with subscript 2 for 2% of polysorbate 80 and A stands for aceclofenac).

2. Materials and methods

2.1. Materials

ACF was purchased from Jinan Jiaquan Chemical Co., Ltd. (Jinan, China). Ryoto® sugar esters, SP P-1670 (approximately 80% monoester, 17% diester and 3% triester) and SS S-970 (approximately 48% monoester, 34% diester, 14% triester and 4% tetraester) were generously gifted by Mitsubishi-Kagaku Foods Corporation (Tokyo, Japan). Egg lecithin (Lipoid E 80) was provided by Lipoid GmbH (Ludwigshaften, Germany). P80 and butylhydroxytoluene (BHT) were supplied by Sigma-Aldrich Laborchemikalien GmbH (Seelze, Germany). Medium chain triglycerides (MCT) (Saboderm TCC) were obtained from Sabo S. p. A (Levate, Italy). Castor oil was purchased from Sigma-Aldrich Chemie GmbH (Steinheim, Germany). Ultrapure water was obtained using GenPure purification system (TKA Wasseranfbereitungssysteme GmbH, Neiderelbert, Germany). All other chemicals were of pharmaceutical or HPLC grade and were used as received without purification. AdminPatch® 600 microneedle array (187 microneedles over 1 cm^2; microneedle height 500 µm) made of stainless steel were provided by AdminMed (Sunnyvale, CA, USA).

2.2. Nanoemulsion preparation

Nanoemulsions were prepared by hot (50 °C) high pressure homogenization (HPH) according to recently described procedure (Isailović et al., 2016). Briefly, the oil phase (20%, w/w) containing a mixture of

MCT and castor oil at a mass ratio of 1:1, egg lecithin and BHT was heated under slight magnetic stirring until complete dissolution of lecithin was achieved, and afterward, ACF (1%, w/w) was added. The prepared oil phase was then mixed with the equally heated aqueous phase (50 °C) consisted of ultrapure water and SP and/or SS or P80 and further pre-homogenized with a rotor-stator homogenizer Ultra-Turrax® T25 digital (IKA® Werke GmbH & Company KG, Staufen, Germany) at 8000 rpm for 3 min. The obtained coarse emulsions were subsequently homogenized with a high pressure homogenizer Emulsi-Flex-C3 (Avestin Inc., Ottawa, Canada) at 800 bar for 20 or 10 homogenization cycles (depending on coemulsifier used). The obtained nanoemulsions were stored in headspace glass vials with crimp cups at room temperature (25 ± 2 °C) and in a fridge (4 ± 1 °C) for one year. Detailed composition of the investigated nanoemulsions is given in Table 1.

2.3. Nanoemulsion characterization

2.3.1. Particle size analysis

The mean droplet size (intensity weighted mean diameter, Z-ave) and polydispersity index (PDI) of monitored nanoemulsions were determined by photon correlation spectroscopy (PCS), using a Zetasizer Nano ZS90 (Malvern Instruments Ltd., Worcestershire, UK). Prior to measurements, nanoemulsion samples were diluted with ultrapure water (1:1000, v/v) to obtain optimum scattering intensity. The measurements were carried out at 25 °C at a fixed scattering angle of 90° using a He-Ne laser at 633 nm.

2.3.2. Zeta potential

Zeta potential (ZP), as a measure of droplet surface charge, was determined using Zetasizer Nano ZS90 (Malvern Instruments Ltd.). The measurements were conducted at 25 °C, immediately upon appropriate dilution of nanoemulsion samples (1:500, v/v) with electrolyte solution consisted of ultrapure water with constant conductivity adjusted to 50 μS/cm by 0.9% (w/v) sodium chloride solution.

2.3.3. pH value

The pH values of investigated nanoemulsions were determined using a HI9321 pH meter (Hanna Instruments Inc., Michigan, USA). The measurements were conducted at 25 °C by simply plunging the pH meter glass electrode into the samples.

2.3.4. Chemical stability of aceclofenac

The content of ACF and its main degradation product, diclofenac (DIC), was monitored in the course of one year for all selected nanoemulsions stored in the fridge (4 ± 1 °C). Briefly, a 100 μl volume of nanoemulsion was diluted in methanol and the resulting solution was injected in the UHPLC-MS. Detailed description of UHPLC-MS method utilized for determination of ACF/DIC content was recently published by our group (Isailović et al., 2016).

2.4. In vitro release study

In vitro release test was performed using modified Franz diffusion cells (Gauer Glas, D-Püttlingen, Germany) with a receptor volume of 12 ml and an effective diffusion area of 2.01 cm^2. Degassed, pre-heated phosphate buffer saline pH 7.4 (PBS) was placed in the receiver compartments and continuously stirred with a magnetic stirrer at 500 rpm. Polycarbonate membranes (Nuclepore™, Whatman, Maidstone, United Kingdom), previously soaked in PBS for 12 h, were carefully clamped between donor and receptor chambers, ensuring that no air gaps were formed. The investigated nanoemulsions (500 μl) were carefully spread on the entire membrane in the cavity of the donor compartments, which were then capped with Parafilm™ to prevent any evaporation. The temperature of diffusion cells was maintained at 32 ± 0.5 °C throughout the experiment, by means of circulating water bath. At predetermined time points over 6 h, aliquots (0.6 ml) of receptor medium were withdrawn and immediately replaced with the equal volume of fresh, thermostated PBS. The amount of ACF released was determined using previously reported UHPLC-MS procedure (Isailović et al., 2016). In order to determine the in vitro release rate of ACF from each investigated formulation, the cumulative amount of ACF released per cm^2 of the exposed area was plotted against the square root of time.

2.5. In vitro skin permeation study

In vitro permeation study was carried out using modified Franz diffusion cells and dermatomed pig ear skin as a membrane, by employing the experimental conditions as identical as possible to the test conditions utilized for in vitro release study. Porcine ears obtained from the local abattoir immediately after slaughter (before scalding) were carefully washed under cold running water, blotted dry with the soft tissue and the skin of the outer side was excised using a scalpel. The full-thickness skin was then cleaned off with isotonic saline and cotton swabs, blotted dry with a soft tissue, wrapped in the aluminum foil and stored at −20 °C within one month. On the day of the experiment, after thawing at room temperature, hairs were shortened with scissors, the skin was dermatomed to a thickness of 1 mm (Dermatom GA 630; B. Braun Melsungen AG, Melsungen, Germany) and punched to the discs with a diameter 25 mm. Afterwards, each receptor chamber was filled with degassed, pre-heated PBS. The pig ear skin was mounted between the donor and receptor chambers, with SC facing the donor compartment, and was allowed to equilibrate for 30 min. Thereafter, 500 μl of investigated nanoemulsions was carefully applied on the membrane in donor chambers, which were then covered with occlusive Parafilm™. Cumulative amount of drug permeating per unit area (mg/cm^2) over 45 h were plotted against time, and then permeation rate (steady state flux) was determined from the slope of linear portion of the plot for each investigated formulation. Permeation coefficients (mg/cm^2 h) were calculated by dividing permeation rates (μg/cm^2 h) by initial concentration of ACF in the vehicle (μg/mg).

2.6. Differential stripping

In order to assess the contribution of follicular uptake in overall skin penetration of ACF from investigated nanoemulsions, differential stripping was performed in vitro, using porcine ear skin. Opposite to in vitro permeation procedure where the skin was excised from the porcine ears, in this case, the skin remained on the cartilage during the experiment. Namely, after washing under cold running water, porcine ears were blotted dry with the soft tissue, wrapped in the aluminum foil and stored at −20 °C until use (within one month). On the day of experiment, after defrosting, hairs were shortened with scissors and ears with immaculate skin surface were fixed on styrofoam plates. When transepidermal water loss (TEWL) reached the values of approximately 15 $g^{-2} h^{-1}$ (measured using a Tewameter® TM 210, Courage + Khazaka, Köln, Germany) (Klang et al., 2012), investigated formulations (15 μl/cm^2) were carefully distributed on assigned skin sites with or without massage, depending on the experimental setup. Massage was performed by the gloved forefinger of one well-trained person (to minimize deviation), with a circular motion for 3 min and a pressure of ~2 N (controlled by the balance). After a 1 h incubation period, the residual formulations were gently removed with dry cotton swabs, and 15 adhesive D-squame® discs (CuDerm Corporation, USA) were utilized for sequential removal of SC layers. The adhesive tapes were pressed onto the skin using a roller device (300 g) to minimize the influence of the skin wrinkles and furrows. Afterwards, two cyanoacrylate skin surface biopsies were performed, putting a drop of cyanoacrylate superglue (UHU GmbH & Co. KG, Brühl, Germany) in the center of each treated site and covering it with adhesive tape using a roller. The superglue was allowed to polymerize for 10 min, and then, adhesive tape with the dried cyanoacrylate was quickly removed,

containing mainly the follicular content of ACF. After removal of SC layers, each tape was transferred into a centrifuge tube and ACF was extracted with 4 ml of ethanol (70%, v/v). The tubes were sonicated (Sonorex RK 120H, Bandelin, Berlin, Germany) for 15 min and then centrifuged at 4000 rpm for 5 min (Centrifuge MPW-56; MPW Med. Instruments, Warszawa, Poland). On the other hand, the cyanoacrylate surface biopsies were extracted with 4 ml of acetonitrile using ultrasound for 15 min and centrifugation for 15 min at 4000 rpm. Obtained supernatants were immediately analyzed for ACF content using UHPLC-MS method (Isailović et al., 2016).

2.7. In vivo pharmacokinetic study

In order to assess the efficiency of selected SE-based nanoemulsion in comparison with conventional P80-based one, together with the effect of skin microneedle pretreatment, the in vivo pharmacokinetic study was performed in Wistar rats (Military Farm, Belgrade, Serbia). The study was conducted in accordance with EEC Directive 86/609 and was approved by the Ethical Committee on Animal Experimentation of the Faculty of Pharmacy, University of Belgrade, Serbia. The rats were housed in plastic cages on a 12 h light/dark period, under controlled laboratory conditions – temperature (22 ± 1 °C), relative humidity (40–70%) and illumination (120 lx). All animals were provided with pellet food and tap water ad libitum.

The rats were equally divided into five groups (3 for each): groups 1 and 2 – topical application of SP-based nanoemulsion, with and without skin pretreatment with stainless steel microneedles, respectively; groups 3 and 4 – topical application of P80-based nanoemulsion, with and without skin pretreatment with microneedles, respectively; group 5 – intravenous (i.v.) application of ACF solution (25% of ethanol (96% v/v) and 75% of the phosphate buffer, pH = 7.4).

Briefly, on the day of experiment, animals were lightly anesthetized by intraperitoneal (i.p.) injection of ketamine (10% Ketamidor, Richter Pharma Ag, Wels, Austria) and the hair of upper back region was carefully shaved with an electric clipper. In order to prevent formulation leakage, a plastic ring, delimitating the area of 2.01 cm^2, was immediately fixed to a shaved region using cyanoacrylate superglue. Afterwards, 500 µl of investigated formulations were applied and reservoirs were tightly covered with the silicone film (Parafilm™, USA). In the groups pre-treated with microneedles (groups 2 and 4), before sticking the plastic ring, microneedle array was pressed into the rat skin using a home-made applicator which enabled uniform insertion force. After 1 min, microneedle array was removed and punctured skin was immediately treated with investigated formulations. Finally, in the group 5 intended for i.v. administration, ACF solution was infused into the tail vein using a syringe pump (Stoelting Co., Wood Dale, USA).

At predetermined time intervals, the blood samples (no > 200 µl per time point) were collected from the tail vein into heparinized tubes and centrifuged at 3000 rpm for 15 min using a Eppendorf MiniSpin® plus centrifuge (Westbury, NY, USA) to obtain plasma. The ACF and its metabolite DIC were extracted using the procedure recently reported by Todosijević et al. (2015). Briefly, 100 µl of rat plasma, 25 µl of methanol and 200 µl of acetonitrile were placed into centrifuge tubes and vortexed for 60 s. Afterwards, the diluent (methanol and ultrapurified water in the mixture of 80:20, v/v), was added up to 1 ml and, after vortexing for 60 s, the resulting solution was centrifuged at 10,000 rpm for 10 min. Calibration standards were prepared by addition of 5 µl of the working standard solutions (containing 1, 2, 5, 10, 20, 30 and 50 µg/ml of ACF and the same concentration of DIC using methanol) into 95 µl of plasma, followed by the extraction procedure described above. The supernatant was separated and analyzed using UHPLC-MS method (Isailović et al., 2016).

At the end of experiment, in order to determine the amount of ACF and DIC retained in the skin, the rats were sacrificed using i.p. injection of ketamine. The residual formulations were then carefully removed and full-thickness skin treated with investigated samples was carefully excised from each animal. After cutting, small pieces of skin were transferred into 5 ml of methanol and shaken for 24 h at room temperature for complete extraction of ACF and DIC. The resulting mixture was centrifuged at 3000 rpm for 30 min and obtained supernatant was immediately analyzed for drug content using UHPLC-MS method (Isailović et al., 2016).

Non-compartmental pharmacokinetic analysis was performed using PK Functions for Microsoft Excel software (Usansky, Desai and Tang-Liu, Department of Pharmacokinetics and Drug Metabolism, Allergan, Irvine, CA; http://www.boomer.org/pkin/soft.html). The following pharmacokinetic parameters of ACF were calculated: maximum plasma concentration (C_{max}), time to reach the maximum plasma concentration (T_{max}) and area under the plasma concentration–time curve from time zero to last measurable time point ($AUC_{0–24h}$). The absolute bioavailability (F_{abs}) of ACF following transdermal administration of ACF in nanoemulsions, with and without skin perforation with solid microneedles was determined relative to the i.v. solution using the formula: $F = AUC_{0–24h,ACF\ nanoemulsion} / AUC_{0–24h,ACF\ solution}$.

2.8. Statistical analysis

Whenever applicable, the results were presented as mean ± standard deviation (SD). Statistical analysis was performed using Student's *t*-test or nonparametric Mann–Whitney *U* test for pairwise comparisons as well as one-way analysis of variance (ANOVA) followed by post hoc Tukey's HSD test, depending on the nature of the data (PASW Statistics version 18.0, SPSS Inc., Chicago, USA). An assessment of the normality of data was carried out using the Shapiro–Wilk test. Statistical significance was set at $p < 0.05$.

3. Results and discussion

3.1. Physicochemical characterization and stability testing

Considering a number of pharmacological concerns associated with oral administration of ACF, our research group has recently proposed a newer approach involving biocompatible lecithin-based nanoemulsions as alternative vehicles for delivering this, quite challenging NSAID, via skin. Owing to weak acidic character (pKa = 4.7 (Todosijević et al., 2015)), ACF is, at least partly, negatively charged at the formulation pH and subsequently, shows the surface activity. Hence, being preferentially located at the interface (Isailović et al., 2016), ACF may interact strongly with the phospholipid film at the droplet surface, thus affecting nanoemulsion stability. The addition of spacious surface-active agent(s), enabling the formation of complex close-packed interfacial film at the droplet surface and/or additional steric stabilization of dispersed nano-droplets, could be a promising strategy to optimize the storage stability of ACF-loaded nanoemulsions (Klang and Valenta, 2011; Klang et al., 2015). Accordingly, taking into account previous preliminary experiments (Isailović et al., 2016), in this study, we have focused on the three most promising lecithin-based nanoemulsions of ACF containing SP and/or SS as coemulsifiers (L_2P_2A, $L_{1.5}S_{0.5}P_2A$, $L_1S_1P_2A$), with favorable physicochemical properties (Z-Ave 180.2 ± 1.2 nm, PDI 0.111 ± 0.008, ZP –41.5 ± 2.7 mV, pH 3.5 ± 0.3), as well as on the P80-costabilized one (L_2P80_2A) as the reference (Z-Ave 187.6 nm, PDI 0.120, ZP –34.6 mV, pH 3.7), and reported, for the first time, their long-term stability.

Firstly, it should be emphasized that physicochemical stability of ACF-loaded nanoemulsion samples was greatly affected by the storage conditions as well as emulsifier mixture composition. Namely, after one-year storage, the visual inspection showed phase separation (irreversible upon gentle agitation) and/or droplet size increase accompanied with the loss of bluish tint and obviously increased viscosity for tested ACF-loaded nanoemulsions stored at room temperature (25 ± 2 °C). Contrary, samples stored at 4 ± 1 °C were highly fluid and homogeneous with milky-white appearance with the bluish touch,

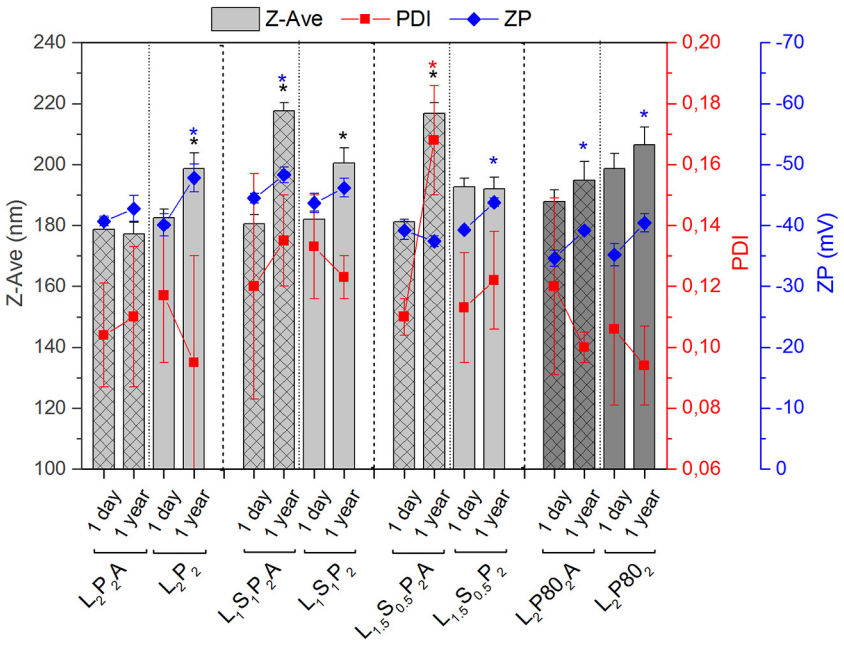

Fig. 1. Droplet size (Z-ave), polydispersity index (PDI) and zeta potential (ZP) of optimized sucrose ester-based nanoemulsions (L_2P_2A, $L_{1.5}S_{0.5}P_2A$, $L_1S_1P_2A$), polysorbate 80-based one (L_2P80_2A) and corresponding placebo nanoemulsions (L_2P_2, $L_{1.5}S_{0.5}P_2$, $L_1S_1P_2$, L_2P80_2) one day after preparation and after one-year storage at 4 ± 1 °C (mean ± SD, n = 3); *p < 0.05 compared to the same sample one day after preparation.

just like after preparation, suggesting satisfying long-term physical stability. Therefore, only the results of droplet size, PDI and ZP measurements for ACF-loaded nanoemulsions and corresponding placebo samples stored in the fridge (4 ± 1 °C) for a year are presented in Fig. 1. The mean droplet size and size homogeneity of ACF-loaded nanoemulsions co-stabilized by hydrophilic coemulsifiers – SP and P80 (L_2P_2A, L_2P80_2A) remained practically unchanged during the storage period. On the other hand, the addition of SS with intermediate lipophilicity in the mixture employed for nanoemulsion stabilization ($L_{1.5}S_{0.5}P_2A$, $L_1S_1P_2A$) led to reorganization of surfactants' molecules at the droplet surface, causing statistically significant increase in droplet size (*t*-test, $p < 0.05$) compared to initial values. In addition, after one-year storage, the tested ACF formulations showed highly negative ZP values ranged from −37 to −48 mV (Fig. 1), reflecting sufficiently high surface charge for droplet-droplet repulsion and consequently, satisfying stability against coalescence. However, it is important to note that ZP of all ACF-loaded nanoemulsions slightly increased during storage. Considering that the comparable tendency was observed for the corresponding placebo samples, this increase could not be ascribed to the presence of ACF, but rather to the hydrolytic degradation of phospholipids and oils, and, the formation of free fatty acids. As a result, significant pH drop (approximately 0.5 units) was also recorded, but all obtained values were still within the admissible limits for topical preparations (3.04, 3.08, 3.29, 3.09 for L_2P_2A, $L_{1.5}S_{0.5}P_2A$, $L_1S_1P_2A$, L_2P80_2A, respectively). Additionally, the average content of ACF remained around 90% for all tested nanoemulsions stored at 4 ± 1 °C (DIC content was around 10%), suggesting that the drug incorporation into nanoemulsion oil phase and interfacial phospholipid layer in combination with appropriate storage conditions can maintain the chemical stability of drug (Baspinar et al., 2010). Interestingly, the average content of ACF and its main degradation product DIC in nanoemulsion samples stored at 25 ± 2 °C was remarkably changed (139.0–171.3% and 17.1–34.2%, respectively) in the course of one year. However, observed variations in ACF/DIC content could be rather attributed to observed physical instability (droplet size increase) of tested nanoemulsions and methodological limitations, than to the chemical instability of ACF. Overall, such findings may preliminary imply the necessity of appropriate storage conditions for this type of formulation, i.e., keeping at fridge temperature (2–8 °C).

In case of blank nanoemulsions, minor variations in the monitored physicochemical parameters were detected within one year of storage at 4 ± 1 °C, following generally similar trends observed for corresponding ACF-loaded nanoemulsions (Fig. 1). Combining investigated stability parameters, we can conclude that, despite the low pH value, developed ACF-loaded nanoemulsion stabilized by lecithin/SP exhibited satisfying physicochemical stability comparable to the reference stabilized by lecithin/P80 mixture during one year at 4 ± 1 °C (and even longer), probably owing to: 1) steric shielding effect of employed non-ionic surfactants that together with lecithin form layer of sufficient thickness and density at the droplet surface; 2) increased viscosity of this coating layer with decreased storage temperature (Li and Lu, 2016). On the other hand, considering that PCS is regarded as a very sensitive mean for detecting nanoemulsion instability (Müller et al., 2012), observed size increase (> 20 nm) of nanoemulsions containing SS in the stabilizer mixture may point out to their compromised long-term stability.

3.2. In vitro release study

Considering that (trans)dermal drug delivery is a multistep process involving release of active drug substance from the formulation applied onto the skin surface and penetration/diffusion of the drug into or through the skin to the systemic circulation before eliciting the desired pharmacological effect, firstly, an assessment of in vitro ACF release from investigated nanoemulsions was carried out using vertical diffusion cells and synthetic polycarbonate membranes (with average pore size of 100 nm to prevent the entrance of nanodroplets into the receptor chamber). Although not directly predictive of drug bioavailability in vivo, generated in vitro release data may reflect both the structural behavior of tested formulations and possible drug–carrier interactions, thus potentially contributing to more accurate understanding of the complexity of factors involved in delivery of ACF into/through the skin from investigated nanoemulsions (Morais and Burgess, 2014).

Obtained release profiles of ACF and corresponding in vitro release parameters are displayed in Fig. 2 and Table 2, respectively. Firstly, as can be seen in Fig. 2, when the cumulative amount of ACF released per unit area was plotted against the square root of time, a linear relationship ($r > 0.99$) was obtained for all tested nanoemulsion formulations, implying that ACF release follows the Higuchi diffusion model. Secondly, it is obvious that novel SE-based nanoemulsions significantly enhanced the release rate of ACF (ANOVA, $p < 0.05$) as well as the cumulative amount of ACF released at the end of experiment

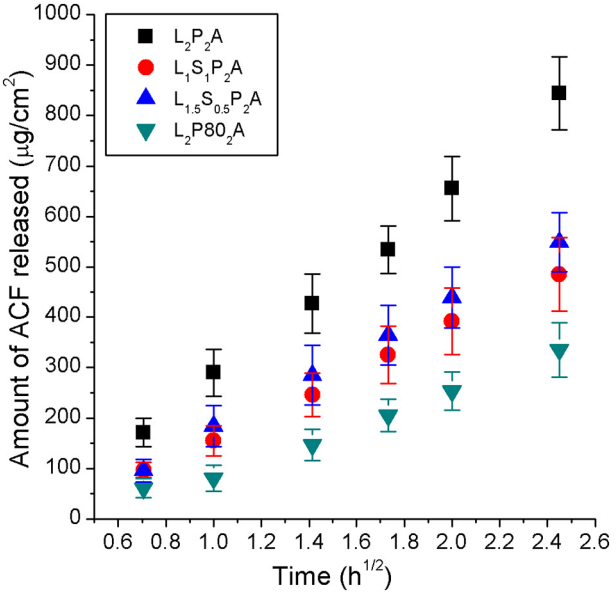

Fig. 2. In vitro release profiles of aceclofenac (ACF) from the investigated formulations determined across the synthetic polycarbonate membrane (pore size 100 nm) using vertical diffusion cells (mean ± SD, n = 5).

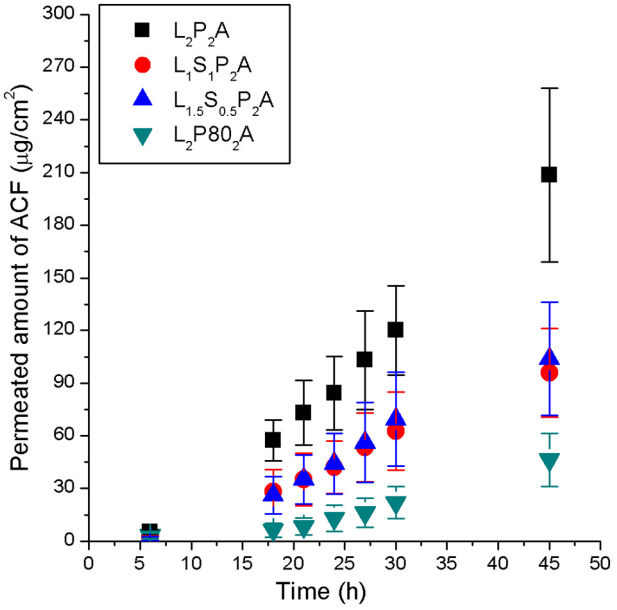

Fig. 3. In vitro permeation profiles of aceclofenac (ACF) determined across the dermatomed pig ear skin (mean ± SD, n = 5) reflecting the influence of differences in emulsifier mixture composition on the in vitro skin absorption of ACF.

Table 2
Release and permeation parameters obtained through in vitro characterization across the polycarbonate membrane and dermatomed pig ear skin, respectively (mean ± SD, n = 5).

Sample	Release rate (μg/cm² h)	Permeation rate (μg/cm² h)	Permeation coefficient (mg/cm² h)
L_2P_2A	379.65 ± 33.91*	5.76 ± 1.32*	0.58 ± 0.13*
$L_{1.5}S_{0.5}P_2A$	258.23 ± 26.26	2.75 ± 0.74	0.28 ± 0.07
$L_1S_1P_2A$	226.83 ± 39.94	2.52 ± 0.62	0.25 ± 0.06
L_2P80_2A	162.78 ± 33.01#	1.59 ± 0.40#	0.16 ± 0.04#

* $p < 0.05$ compared to $L_{1.5}S_{0.5}P_2A$, $L_1S_1P_2A$ and L_2P80_2A.
\# $p < 0.05$ compared to L_2P_2A, $L_{1.5}S_{0.5}P_2A$ and $L_1S_1P_2A$.

(ANOVA, $p < 0.05$), compared to the reference nanoemulsion (Table 2). Since all tested nanoemulsions had similar droplet size (~180 nm), pH value (~3.5) and viscosity (~3.5 mPa s) (Isailović et al., 2016), with the same total concentration of surfactants (4%, w/w) and equal quantity of ACF (1%, w/w), the lowest release of ACF from L_2P80_2A formulation could be attributed to the differences in the structure of employed cosurfactants as well as in their packing at the droplet surface (Montenegro et al., 2012). Namely, based on obtained results, it seems that P80, despite the branched hydrophilic region, can form a more closely packed layer at the oil-water interface, resulting in the lowest release of ACF among all formulations examined. However, the release-enhancing effect of SEs per se also could not be ignored, since there is certain evidence in the literature showing that SEs are capable to improve the release of poorly water-soluble drugs (Szűts and Szabó-Révész, 2012).

Looking strictly at the results obtained for SE-based nanoemulsions, the release rate and total quantity of ACF released from L_2P_2A were significantly higher (ANOVA, $p < 0.05$) than from $L_{1.5}S_{0.5}P_2A$ and $L_1S_1P_2A$ formulations containing SS as additional coemulsifier (Table 2). Considering that SS contains the significant amount of more lipophilic sucrose diesters, increasing content of SS in the blend at the expense of lecithin content reduction probably resulted in a more dense packing of surfactant tails, causing increased rigidity of the surfactant layer (Aramaki et al., 2001) and, consequently, the lower release of ACF. Also, it is interesting to note that SEs of shorter fatty acid and higher HLB value (SP in our case) may increase drug release more than SEs of longer fatty acids and lower HLB value (SS) (Csóka et al., 2007). Therefore, based on obtained results, it could be deduced that the type and proportion of surfactants employed for nanoemulsion stabilization play an important role in the ACF release.

3.3. In vitro permeation study

Bearing in mind that synthetic membranes are unable to reflect the complex interactions between the skin and nanoemulsion excipients, a rational approach for designing and optimizing skin formulations aimed for (trans)dermal drug delivery requires the use of well-defined skin model, which can permit to detect potentially meaningful differences regarding the rate and extent of drug delivery through the skin. Hence, owing to the numerous anatomical, histological and physiological similarities with human skin (Flaten et al., 2015), porcine ear skin was used as a good alternative model to compare skin absorption of ACF from tested formulations.

The cumulative permeation profiles of ACF and corresponding in vitro permeation parameters are presented in Fig. 3 and Table 2, respectively. As the graph shows (Fig. 3), permeation behavior of ACF was closely related to the nature of surfactants utilized for nanoemulsion preparation. The reference sample stabilized by egg lecithin/P80 combination showed the lowest quantity of ACF permeated during 45 h and was accompanied with the lowest value of steady-state flux and permeation coefficient (Table 2). On the other hand, all three SE-based nanoemulsions significantly improved (ANOVA, $p < 0.05$) the amount of ACF permeated in 45 h, whereby L_2P_2A sample has promoted the highest delivery of ACF (Fig. 3), simultaneously showing the highest steady-state flux and permeation coefficient (Table 2). The incorporation of additional surfactant, SS, significantly reduced the permeation rate of ACF (no difference was found between $L_{1.5}S_{0.5}P_2A$ and $L_1S_1P_2A$ formulations). Considering that these results were in good agreement with the release profiles of ACF from the investigated nanoemulsions, it appears that the release was a key factor determining the ACF uptake through the dermatomed pig ear skin. However, it should be kept in mind that there is substantial evidence showing that SEs can increase skin permeability by disturbing the densely packed lipids which fill the

extracellular space of the SC, thus allowing easier drug diffusion through the skin (Hoeller et al., 2009; Szűts and Szabó-Révész, 2012). Also, nanodroplets, depending on the composition of the stabilizer film, may penetrate into the hair follicles to considerable extent, thus affecting skin absorption of ACF. In the other words, the observed enhancement in ACF permeation from developed SE-based nanoemulsions could not be ascribed only to the enhanced release of ACF, since SEs as penetration enhancers, as well as follicular uptake of nanodroplets, can take a part. Therefore, in order to identify the preferable factors contributing to improved delivery of ACF through the skin, L_2P_2A and L_2P80_2A nanoemulsions were submitted to the differential stripping study. Formulations containing SS were excluded from the further investigations because of their compromised long-term stability and deteriorated release/permeation of ACF when compared to the formulation containing only egg lecithin and SP as stabilizers.

3.4. Differential stripping

In order to quantify the amount of ACF localized in the SC and hair follicles, differential stripping, combining conventional tape stripping processes with cyanoacrylate skin surface biopsy, was performed on the porcine ear skin. Despite the certain anatomical differences between human and porcine hair follicles, an excellent in vitro–in vivo correlation between both models was demonstrated, supporting the suitability of the pig ear for quantifying drug uptake into the hair follicles (Raber et al., 2014). In this regard, it is important to emphasize that results of previously conducted preliminary study indicated that removal of 15 tape strips is sufficient to remove ACF localized in the SC (after the 15th tape strips, amount of ACF removed from the areas of porcine ear treated with tested formulations was negligibly low). Hence, amount of ACF extracted from the cyanoacrylate biopsies can be defined as the amount present in hair follicles.

As the graph shows (Fig. 4), ACF was taken up in the SC to the higher extent from SP-based nanoemulsion than from the reference P80-based one, but, due to the high variability of obtained data, the observed differences were not statistically significant (*t*-test, $p > 0.05$). Interestingly, in vivo, in human volunteers, the total quantity of ACF recovered in the SC from L_2P_2A was significantly higher (t-test, $p < 0.05$) than from the formulation L_2P80_2A (Isailović et al., 2016). In other words, although no statistically significant difference was detected between tested formulations using pig ear in vitro model, the trend observed in vivo was predicted correctly, proving that the pig ear is a suitable model for quantifying drug penetration into the skin (Raber et al., 2014). Massage applied during administration of the investigated nanoemulsions did not markedly affect the ACF uptake in the SC. Notably, the levels of ACF recovered from the hair follicles were appreciably lower than those found in the SC and no statistically significant difference (t-test, $p > 0.05$) could be determined between tested formulations (Fig. 4). Three-minute massage of porcine ear prior to the one-hour incubation period generally increased follicular uptake of ACF from both nanoemulsions, but more pronounced improvement of ACF follicular penetration was detected in case of L_2P80_2A. This finding confirms that mimicking the natural movement of the hair by skin massaging improves the transport of nanodroplets into the hair shaft (Mathes et al., 2016). However, taking into account all obtained results, it appears that the intercellular route was the predominant diffusion route of ACF, i.e., contribution of transfollicular pathway in overall skin penetration of ACF from tested nanoemulsions was relatively small. In other words, perturbation of the SC barrier by egg lecithin and SP and/or improved ACF release could be considered responsible for observed enhanced delivery of ACF through the porcine ear skin from L_2P_2A nanoemulsion relative to the reference sample.

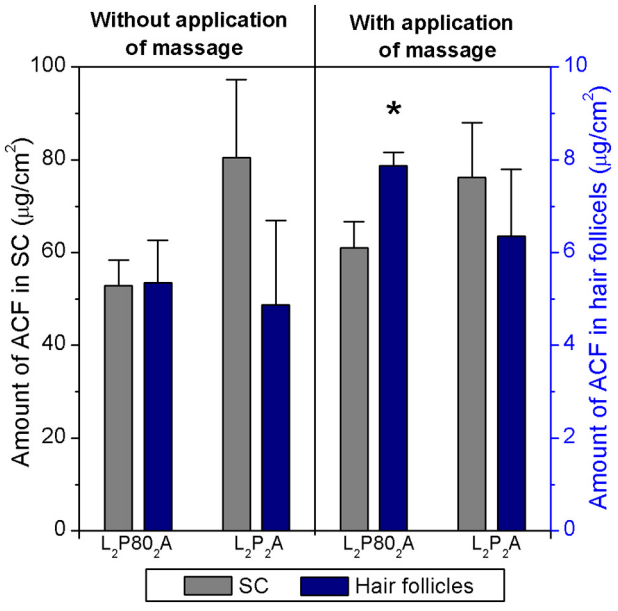

Fig. 4. Total amount of aceclofenac (ACF) penetrated in the stratum corneum (SC) and hair follicles of porcine ear skin, with and without massage applied during administration of tested nanoemulsions (mean ± SD, n = 3); *$p < 0.05$ compared to the value obtained without application of massage.

3.5. In vivo pharmacokinetic study

In order to examine whether the poorly water-soluble ACF could be successfully delivered systemically from developed nanoemulsions per se or combined with the SC pretreatment using solid microneedles (physical enhancing effect), and to uncover the specific role of coemulsifier type in drug delivery into and through the skin in vivo, the pharmacokinetic studies (including determination of ACF amount deposited in the skin) were performed in rats. Although the use of hairy rat skin is restricted in in vitro permeation studies, the rats are commonly utilized in in vivo pharmacokinetic studies for the assessment of transdermal drug delivery systems, due to their small size, uncomplicated handling and relatively low cost (Choi et al., 2012). Furthermore, Yu et al. (2014) observed good linear correlations ($r > 0.9$) between rat plasma AUC and cumulative amount of metronidazole permeated across the pig skin from the corresponding nanoemulsion and gel formulations. Having in mind recently published data on successful delivery of various drugs across the skin (e.g., Kaur et al., 2014; Modepalli et al., 2015), commercially available microneedles (AdminPatch® microneedle arrays) with a needle height of 500 μm were utilized to create micropores in the outer skin layers before application of nanoemulsion samples, simultaneously avoiding the blood capillaries located deeper the dermis and pain receptors. Additionally, it is important to note that AdminPatch® microneedle arrays are made from the stainless steel which is biocompatible and has been used to create needles (i.e. hypodermic needles) for decades. Furthermore, owing to good mechanical properties of stainless steel, the risk of occasional breakage of microneedle tips upon insertion into skin is small (Kim et al., 2012; Maaden et al., 2012). The mean plasma concentration-time profiles of ACF from tested nanoemulsions, with and without skin perforation with microneedles, are presented in Fig. 5, whereas the relevant pharmacokinetic parameters obtained following topical application of ACF nanoemulsions and intravenous administration of ACF solution are summarized in Table 3.

As the graphs show (Fig. 5), after administering both ACF-loaded nanoemulsions (L_2P_2A and L_2P80_2A), a slight gradual increase in the plasma concentrations of ACF was observed within the initial time points (0.5–6 h after application onto the skin surface), with the maximal concentrations achieved at 24 h post-skin application (Table 3), suggesting relatively slow absorption into systemic circulation. Taking into account the proposed localization of ACF in the tested

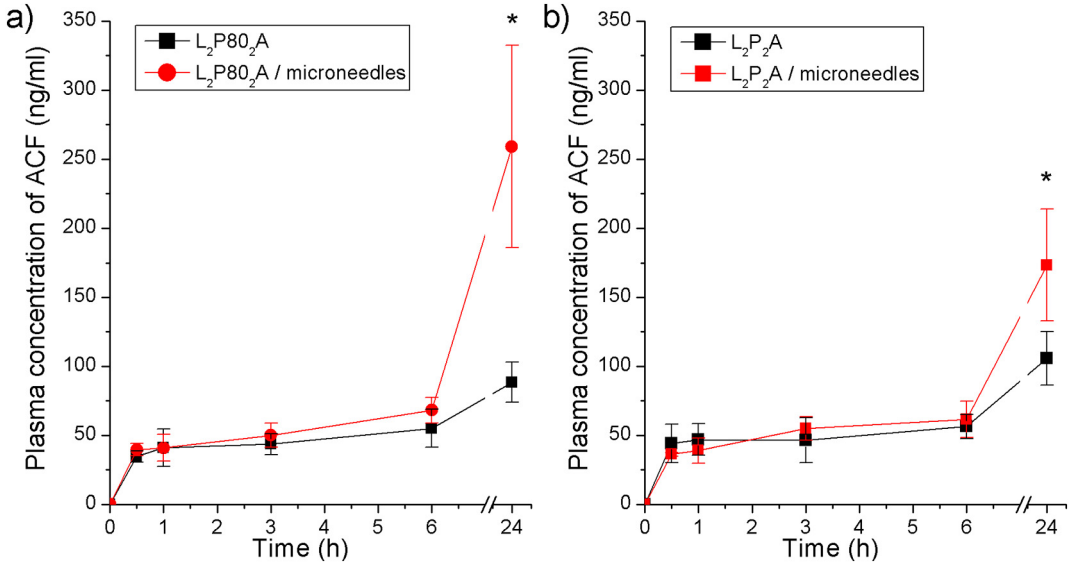

Fig. 5. Plasma concentration–time profiles of aceclofenac (ACF) after transdermal administration of selected nanoemulsions, with (b) and without (a) skin perforation with stainless steel microneedles (mean ± SD, n = 3); *p < 0.05 compared to value obtained without skin perforation with microneedles.

nanoemulsions (Isailović et al., 2016), delayed absorption of ACF could be explained by the time needed for ACF release from the oil/interface to the aqueous phase of nanoemulsion in the sufficient quantity, as well as for its penetration/diffusion into/through the skin before it is taken up by the blood vessels. Although the mean plasma concentrations of ACF tended to be slightly higher with L_2P_2A nanoemulsion, particularly at the last time point, no statistically significant difference (*t*-test, $p > 0.05$) was observed when comparing with P80-costabilized nanoemulsion (L_2P80_2A) (Fig. 5). Likewise, no significant difference (t-test, $p > 0.05$) was found in the mean plasma $AUC_{0–24h}$ between these two formulations (Table 3), further indicating that, in this case, the variation in coemulsifier type employed for nanoemulsion production did not affect ACF bioavailability in vivo. When relating these results to the in vitro permeation findings, it is obvious that results obtained with porcine ear skin in vitro were not completely indicative of those obtained in vivo in rats, probably due to the significant discrepancies in the thickness and hair follicle density between pig and rat skin (Flaten et al., 2015). Having in mind results obtained from differential stripping, it is reasonable to assume that, due to the high density of hair follicles in the rat skin, greater follicular uptake of ACF might be responsible for improved delivery of ACF from P80-based nanoemulsion across the rat skin and hence, for no apparent differences observed between investigated SP-based and P80-based ACF nanoemulsion formulations.

On the other hand, the insertion of microneedle array in the skin surface resulted in a marked increase (Mann–Whitney *U* test, $p < 0.05$) of ACF maximal concentrations (C_{max}) achieved 24 h after administration of both nanoemulsion formulations (Table 3), but no improvement in the mean plasma concentrations of ACF was detected at the initial time points (0.5–6 h post-skin application) (Fig. 5). These results suggest that ACF-loaded nanodroplets can penetrate into the transient microconduits created by microneedles through the SC and viable epidermis, simultaneously confirming that ACF release from nanoemulsion droplets is the important rate-limiting step for its absorption into the systemic circulation. Interestingly, the greater enhancement in the mean plasma $AUC_{0–24h}$ was observed after combining skin perforation by microneedles and L_2P80_2A sample compared to combination of microneedles and L_2P_2A formulation. Namely, as it can be seen from Table 3, $AUC_{0–24h}$ of ACF from P80-based nanoemulsion was 2.1-fold higher for microneedle-treated skin than for intact skin, while in case of SP-based nanoemulsion merely 1.4-fold increase was detected. Therefore, it is reasonable to speculate that nanoemulsion droplet surface, that is, composition of the stabilizer film, was a key factor determining the interaction of nanodroplets with the tissue exposed, thus directly affecting the rate and extent of transdermal drug delivery using microneedle pretreatment (Coulman et al., 2009).

In order to complete the understanding of ACF pharmacokinetics after topical administration of investigated nanoemulsions, with/without skin pretreatment with microneedles, the pharmacokinetic profile of DIC, the major metabolite of ACF in rats (Noh et al., 2015), was of particular interest to this paper as well. After oral administration, DIC plasma concentrations were significantly higher than those of ACF (Noh et al., 2015). In our case, the mean plasma concentrations of DIC at the initial time points (from 0.5 to 6 h after application) were

Table 3
Pharmacokinetic parameters of aceclofenac (ACF) obtained after topical administration of selected nanoemulsions, with and without skin pretreatment with microneedles, as well as after intravenous administration of ACF solution to rats (mean ± SD, n = 3).

Pharmacokinetic parameter	Application route				
	Intact skin		Microneedle-treated skin		Intravenous solution
	L_2P_2A	L_2P80_2A	L_2P_2A	L_2P80_2A	
C_{max} (ng/ml)	105.69 ± 19.53	88.38 ± 14.46	173.37 ± 40.50*	259.23 ± 73.18*	5390.03 ± 725.86[a]
t_{max} (h)	24 ± 0	24 ± 0	24 ± 0	24 ± 0	0
$AUC_{0–24h}$ (h ng/ml)	1648.58 ± 267.22	1541.37 ± 79.40	2399.19 ± 351.38*	3234.81 ± 650.87*	22,149.32 ± 2602.86
F_{abs} (%)	7.44	6.96	10.83	14.60	/

[a] The extrapolated time zero concentration.
* $p < 0.05$ compared to value of corresponding parameter obtained without skin perforation with microneedles.

below the method's limit of quantification (5 ng/ml) for both investigated nanoemulsion formulations, irrespective of the skin treatment with microneedles. Likewise, the mean plasma levels of DIC achieved 24 h after application of both nanoemulsions on intact skin were considerably lower than those of ACF, whereby significantly higher (Mann–Whitney *U* test, $p < 0.05$) DIC concentration was detected after administration of L_2P_2A nanoemulsion (115.98 ± 69.64 ng/ml) compared to L_2P80_2A formulation (17.18 ± 18.82 ng/ml). Additionally, the skin puncturing by microneedle device produced the marked variation in the concentration of DIC achieved 24 h post-skin application of tested samples, showing the more pronounced increase (Mann–Whitney U test, $p < 0.05$) in combination with L_2P_2A formulation (267.06 ± 48.27 ng/ml) relative to L_2P80_2A nanoemulsion (60.68 ± 29.70 ng/ml). It is interesting to note that after intravenous administration of ACF solution, AUC_{0-24h} of DIC was 8-fold higher than that for ACF (data not shown). Therefore, it is obvious that the ratio of plasma ACF and DIC was remarkably changed after topical administration of tested nanoemulsions compared to oral/intravenous delivery, probably as a result of bypassing the extensive metabolism in liver (Wermeling et al., 2008). Likewise, it appears that metabolism of ACF in the rat skin by hydrolyzing enzymes located mainly in the epidermal cells and near to hair follicles (Todosijević et al., 2015) is relatively small.

Absolute bioavailability of ACF (transdermal vs. intravenous administration) from both tested nanoemulsions was < 7.5% (Table 3), suggesting that ACF and its metabolite DIC probably accumulated in the skin and/or diffused into deeper tissues rather than in systemic circulation. Indeed, the considerable amount of ACF was deposited in the rat full-thickness skin within 24 h, but no significant difference (*t*-test, $p > 0.05$) was observed between the investigated formulations (Fig. 6). Depending on the composition of stabilizer film, amount of DIC generated by skin hydrolyzing enzymes, 24 h after dosing, was 6 to 10-fold lower compared to the level of parent drug ACF (Fig. 6). In addition, the amount of DIC retained in the rat skin after application of L_2P_2A formulation was significantly higher (t-test, $p < 0.05$) when compared with L_2P80_2A sample and correlated well with the remarkably higher DIC concentration observed in the systemic circulation (see above). On the other hand, the skin pretreatment with the solid microneedles remarkably (t-test, $p < 0.05$) improved the amount of ACF and DIC deposited in the skin from both tested samples, but more pronounced increase was detected in case of L_2P_2A sample (Fig. 6). Contrary, the absolute bioavailability of ACF was considerably higher after combining the skin perforation by microneedles with P80-based nanoemulsion (14.60%) relative to the SP-based one (10.83%) (Table 3). Hence, it can be concluded that combination of solid microneedles and nanoemulsion co-stabilized by SP may allow the NSAID to achieve higher skin concentrations. On the other side, bearing in mind that the absolute bioavailability 12 h after oral administration of ACF solution was 15% (Noh et al., 2015), our results also demonstrated the significant potential of combining solid microneedles with nanoemulsion costabilized by P80 for enhancing NSAID delivery into the systemic circulation, and therefore, for the effective treatment of various musculoskeletal disorders via transdermal route. However, before drawing further conclusions, it should be kept in mind that maximal plasma concentrations of ACF were detected at the last selected time point (drug elimination phase was not detected), and therefore, further experiments, involving longer monitoring time and larger number of animals, are needed to completely elucidate in vivo fate of ACF from tested nanoemulsions, with and without skin pretreatment with solid microneedles, and to determine whether obtained findings may have clinical relevance and significant influence on ACF therapeutic efficacy.

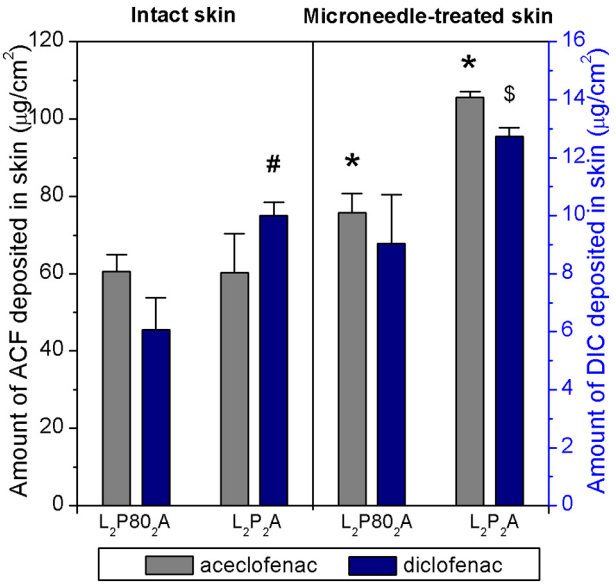

Fig. 6. Amount of aceclofenac (ACF) and diclofenac (DIC) retained in intact and microneedle-treated full-thickness rat skin 24 h after application of tested nanoemulsions (mean ± SD, n = 3); *$p < 0.05$ compared to amount of ACF deposited in the rat skin from corresponding nanoemulsion without skin perforation with microneedles; $^{\#}p < 0.05$ compared to amount of DIC deposited in the rat skin after application of reference nanoemulsion (L_2P80_2A), without microneedle pretreatment; $^{\$}p < 0.05$ compared to amount of DIC deposited in the rat skin from corresponding nanoemulsion without skin perforation with microneedles.

4. Conclusions

The developed ACF-loaded nanoemulsion costabilized by hydrophilic sucrose ester, SP, exhibited the favorable droplet size, narrow size distribution, high surface charge and satisfying long-term stability (at least one year of storage at 4 ± 1 °C), demonstrating similar trend observed for the reference stabilized by widely used lecithin/polysorbate 80 combination. Furthermore, the addition of SP in lecithin-based nanoemulsion markedly improved the rate and extent of ACF release, its penetration into the SC and permeation through the porcine ear skin in vitro, relative to the reference coemulsifier, P80. However, the results obtained in vitro were not completely indicative of the in vivo behavior, since no statistically significant differences were observed between the investigated formulations in ACF pharmacokinetic profile as well as total amount of ACF deposited in the full-thickness rat skin 24 h after dosing, when using nanoemulsions without SC pretreatment with microneedles Additionally, analyzing ACF plasma concentrations in the course of 24 h, it appears that investigated nanoemulsions, irrespective of co-emulsifier type, showed certain potential for delayed drug delivery into the systemic circulation.

In addition, the skin pretreatment with stainless steel microneedles improved ACF delivery into and across the rat skin and finally into the systemic circulation from both tested nanoemulsions. However, obtained results suggested that combination of solid microneedles and SP-costabilized nanoemulsion could be intended for an achievement of higher NSAID skin concentrations, while combination of solid microneedles with nanoemulsion costabilized by P80 could be preferable for enhancing NSAID delivery into the systemic circulation. In other words, it seems that nanoemulsion droplet surface, that is, composition of the stabilizer film, was a key factor determining the rate and extent of dermal/transdermal drug delivery using microneedle pretreatment.

Conflict of interest

The authors have no financial or non-financial interests that represent potential conflict of interests.

Acknowledgement

This work was supported by the projects TR34031 and OI175076, funded by Ministry of Education, Science and Technological Development, Republic of Serbia and the bilateral project between Republic of Serbia and Federal Republic of Germany entitled: *Biosurfactants and biopolysaccharides/film-forming polymers as cosmetic raw materials and prospective pharmaceutical excipients: formulation of colloidal and film-forming delivery systems*. The authors are grateful to Mitsubishi-Kagaku Foods Corporation for supplying sucrose esters.

References

Aramaki, K., Hayashi, T., Katsuragi, T., Ishitobi, M., Kunieda, H., 2001. Effect of adding an amphiphilic solubilization improver, sucrose distearate, on the solubilization capacity of nonionic microemulsions. J. Colloid Interface Sci. 236, 14–19.

Baspinar, Y., Keck, C.M., Borchert, H.H., 2010. Development of a positively charged prednicarbate nanoemulsion. Int. J. Pharm. 383, 201–208.

Cevc, G., Vierl, U., 2010. Nanotechnology and the transdermal route: a state of the art review and critical appraisal. J. Control. Release 141, 277–299.

Choi, J., Choi, M.K., Chong, S., Chung, S.J., Shim, C.K., Kim, D.D., 2012. Effect of fatty acids on the transdermal delivery of donepezil: in vitro and in vivo evaluation. Int. J. Pharm. 422, 83–90.

Coulman, S.A., Anstey, A., Gateley, C., Morrissey, A., McLoughlin, P., Allender, C., Birchall, J.C., 2009. Microneedle mediated delivery of nanoparticles into human skin. Int. J. Pharm. 366, 190–200.

Csóka, G., Marton, S., Zelko, R., Otomo, N., Antal, I., 2007. Application of sucrose fatty acid esters in transdermal therapeutic systems. Eur. J. Pharm. Biopharm. 65, 233–237.

Flaten, G.E., Palac, Z., Engesland, A., Filipović-Grčić, J., Vanić, Ž., Škalko-Basnet, N., 2015. In vitro skin models as a tool in optimization of drug formulation. Eur. J. Pharm. Sci. 75, 10–24.

Friedman, D.I., Schwarz, J.S., Weisspapir, M., 1995. Submicron emulsion vehicle for enhanced transdermal delivery of steroidal and nonsteroidal antiinflammatory drugs. J. Pharm. Sci. 84, 324–329.

Hoeller, S., Sperger, A., Valenta, C., 2009. Lecithin based nanoemulsions: a comparative study of the influence of non-ionic surfactants and the cationic phytosphingosine on physicochemical behaviour and skin permeation. Int. J. Pharm. 370, 181–186.

Isailović, T., Đorđević, S., Marković, B., Ranđelović, D., Cekić, N., Lukić, M., Pantelić, I., Daniels, R., Savić, S., 2016. Biocompatible nanoemulsions for improved aceclofenac skin delivery: formulation approach using combined mixture-process experimental design. J. Pharm. Sci. 105, 308–323.

Jana, S., Manna, S., Nayak, A.K., Sen, K.K., Basu, S.K., 2014. Carbopol gel containing chitosan-egg albumin nanoparticles for transdermal aceclofenac delivery. Colloids Surf. B: Biointerfaces 114, 36–44.

Kaur, M., Ita, K.B., Popova, I.E., Parikh, S.J., Bair, D.A., 2014. Microneedle-assisted delivery of verapamil hydrochloride and amlodipine besylate. Eur. J. Pharm. Biopharm. 6, 284–291.

Khandavilli, S., Panchagnula, R., 2007. Nanoemulsions as versatile formulations for paclitaxel delivery: peroral and dermal delivery studies in rats. J. Invest. Dermatol. 127, 154–162.

Kim, Y.C., Park, J.H., Prausnitz, M.R., 2012. Microneedles for drug and vaccine delivery. Adv. Drug Deliv. Rev. 64, 1547–1568.

Klang, V., Valenta, C., 2011. Lecithin-based nanoemulsions. J. Drug Delivery Sci. Technol. 21, 55–76.

Klang, V., Schwarz, J.C., Lenobel, B., Nadj, M., Auböck, J., Wolzt, M., Valenta, C., 2012. In vitro vs. in vivo tape stripping: validation of the porcine ear model and penetration assessment of novel sucrose stearate emulsions. Eur. J. Pharm. Biopharm. 80, 604–614.

Klang, V., Schwarz, J.C., Valenta, C., 2015. Nanoemulsions in dermal drug delivery. In: Dragicevic, N., Maibach, H. (Eds.), Percutaneous Penetration Enhancers Chemical Methods in Penetration Enhancement. Springer, Berlin, Heidelberg, pp. 255–266.

Larrañeta, E., McCrudden, M.T., Courtenay, A.J., Donnelly, R.F., 2016. Microneedles: a new frontier in nanomedicine delivery. Pharm. Res. 33, 1055–1073.

Li, P.H., Lu, W.C., 2016. Effects of storage conditions on the physical stability of D-limonene nanoemulsion. Food Hydrocoll. 53, 218–224.

Maaden, K., Jiskoot, W., Bouwstra, J., 2012. Microneedle technologies for (trans)dermal drug and vaccine delivery. J. Control. Release 161, 645–655.

Mathes, C., Melero, A., Conrad, P., Vogt, T., Rigo, L., Selzer, D., Prado, W.A., De Rossi, C., Garrigues, T.M., Hansen, S., Guterres, S.S., Pohlmann, A.R., Beck, R.C.R., Lehr, C.M., Schaefer, U.F., 2016. Nanocarriers for optimizing the balance between interfollicular permeation and follicular uptake of topically applied clobetasol to minimize adverse effects. J. Control. Release 223, 207–214.

Milewski, M., Brogden, N.K., Stinchcomb, A.L., 2010. Current aspects of formulation efforts and pore lifetime related to microneedle treatment of skin. Expert Opin. Drug Deliv. 7, 617–629.

Milić, J., Čalija, B., Đorđević, S.M., 2017. Diversity and functionality of excipients for micro/nanosized drug carriers. In: Čalija, B. (Ed.), Microsized and Nanosized Carriers for Nonsteroidal Anti-inflammatory Drugs: Formulation Challenges and Potential Benefits. Elsevier, Academic Press, pp. 95–132.

Modepalli, N., Shivakumar, H.N., Kanni, K.L., Murthy, S.N., 2015. Transdermal iron replenishment therapy. Ther. Deliv. 6, 661–668.

Montenegro, L., Sinico, C., Castangia, I., Carbone, C., Puglisi, G., 2012. Idebenone-loaded solid lipid nanoparticles for drug delivery to the skin: in vitro evaluation. Int. J. Pharm. 434, 169–174.

Morais, J.M., Burgess, D.J., 2014. In vitro release testing methods for vitamin E nanoemulsions. Int. J. Pharm. 475, 393–400.

Müller, R.H., Harden, D., Keck, C.M., 2012. Development of industrially feasible concentrated 30% and 40% nanoemulsions for intravenous drug delivery. Drug Dev. Ind. Pharm. 38, 420–430.

Noh, K., Shin, B.S., Kwon, K.I., Yun, H.Y., Kim, E., Jeong, T.C., Kang, W., 2015. Absolute bioavailability and metabolism of aceclofenac in rats. Arch. Pharm. Res. 38, 68–72.

Raber, A.S., Mittal, A., Schäfer, J., Bakowsky, U., Reichrath, J., Vogt, T., Schaefer, U.F., Hansen, S., Lehr, C.M., 2014. Quantification of nanoparticle uptake into hair follicles in pig ear and human forearm. J. Control. Release 179, 25–32.

Raza, K., Kumar, M., Kumar, P., Malik, R., Sharma, G., Kaur, M., Katare, O.P., 2014. Topical delivery of aceclofenac: challenges and promises of novel drug delivery systems. Biomed. Res. Int. 2014, 406731. https://doi.org/10.1155/2014/406731.

Singh, Y., Meher, J.G., Raval, K., Khan, F.A., Chaurasia, M., Jain, N.K., Chourasia, M.K., 2017. Nanoemulsion: concepts, development and applications in drug delivery. J. Control. Release 252, 28–49.

Szűts, A., Szabó-Révész, P., 2012. Sucrose esters as natural surfactants in drug delivery systems–a mini-review. Int. J. Pharm. 433, 1–9.

Todosijević, M.N., Savić, M.M., Batinić, B.B., Marković, B.D., Gašperlin, M., Ranđelović, D.V., Lukić, M.Ž., Savić, S.D., 2015. Biocompatible microemulsions of a model NSAID for skin delivery: a decisive role of surfactants in skin penetration/irritation profiles and pharmacokinetic performance. Int. J. Pharm. 496, 931–941.

Wermeling, D.P., Banks, S.L., Hudson, D.A., Gill, H.S., Gupta, J., Prausnitz, M.R., Stinchcomb, A.L., 2008. Microneedles permit transdermal delivery of a skin-impermeant medication to humans. Proc. Natl. Acad. Sci. U. S. A. 105, 2058–2063.

Yu, M., Ma, H., Lei, M., Li, N., Tan, F., 2014. In vitro/in vivo characterization of nanoemulsion formulation of metronidazole with improved skin targeting and anti-rosacea properties. Eur. J. Pharm. Biopharm. 88, 92–103.

Zhang, W., Gao, J., Zhu, Q., Zhang, M., Ding, X., Wang, X., Hou, X., Fan, W., Ding, B., Wu, X., Wang, X., Gao, S., 2010. Penetration and distribution of PLGA nanoparticles in the human skin treated with microneedles. Int. J. Pharm. 402, 205–212.